MOX-Report No. 11/2022

A toy model of misfolded protein aggregation and neural damage propagation in neudegenerative diseases

Sampaoli, S.; Agosti, A.; Pozzi, G.; Ciarletta,P.

MOX, Dipartimento di Matematica
Politecnico di Milano, Via Bonardi 9 - 20133 Milano (Italy)

mox-dmat@polimi.it http://mox.polimi.it

A toy model of misfolded protein aggregation and neural damage propagation in neudegenerative diseases.

S. Sampaoli[1], A. Agosti[2], G. Pozzi[1], P. Ciarletta[1*]

[1] MOX Laboratory, Department of Mathematics, Politecnico di Milano, Piazza Leonardo da Vinci 32, 20133 Milano, Italy.

[2] Dipartimento di Matematica 'F. Casorati', Università degli Studi di Pavia, Via Ferrata 5, 27100 Pavia, Italy.

Abstract

Neurodegenerative diseases (NDs) result from the transformation and accumulation of misfolded proteins within the nervous system. They have common features, like the chronic nature and the progressive destruction of neurons in specific areas of the brain. Several mathematical models have been proposed to investigate the biological processes underlying NDs, focusing on the kinetics of polymerization and fragmentation at the microscale and on the spread of neural damage at a macroscopic level. The aim of this work is to bridge the gap between microscopic and

*Corresponding author. E-mail: pasquale.ciarletta@polimi.it

macroscopic approaches proposing a toy partial differential model able to take into account both for the short-time dynamics of the misfolded proteins aggregating in plaques and the long-term evolution of tissue damage. Using the theoretical framework of mixtures theory, we considered the brain as a biphasic material made of misfolded protein aggregates and of healthy tissue. The resulting Cahn-Hilliard type equation for the misfolded proteins contains a growth term depending on the local availability of precursor proteins, that follow a reaction-diffusion equation. The misfolded proteins also posses a chemotactic mass flux driven by gradients of neural damage, that is caused by local accumulation of misfolded protein and that evolves slowly according to an Allen-Cahn equation. The partial differential model is solved numerically using the finite element method in a simple two-dimensional domain, evaluating the effects of the mobility of the misfolded protein and the diffusion of the neural damage. We considered both isotropic and anisotropic mobility coefficients, highlighting that the spreading front of the neural damage follows the direction of the largest eigenvalue of the mobility tensor. In both cases, we computed two biomarkers for quantifying the aggregation in plaques and the evolution of neural damage, that are in qualitative agreement with the characteristic Jack curves for many NDs.

1 Introduction

Neurodegenerative diseases (NDs) such as Alzheimer's disease (AD), Parkinson's disease and amyotrophic lateral sclerosis, result from the transformation and accumulation of specific proteins within the nervous system [1]. They result into a neuronal degeneration that could lead to cognitive impairment, dementia, motor difficulties, psychological and behavioural disorders. Typically NDs have common features, like the chronic and

progressive nature, the destruction of neurons in specific areas of the brain, the damage of the synaptic connections network, and the increase of prevalence with age. Most importantly, they all display a common biochemical origin, that is the accumulation of misfolded protein aggregates [2].

There is experimental evidence that the proteins involved in NDs acquire their pathogenicity by a prion-like mechanism. Indeed, the pathogenic proteins are released by a cell in the extracellular fluid. They later move into other cells, where they act as seeds and induce misfolding of healthy protein [3]. The most important seed-proteins are amyloid-β (involved in senile plaques formation in AD), tau (involved in tauopathies) and α-synuclein (in Lewy-diseases). In physiological conditions the conformation of these proteins ensures the solubility and thus the correct secretion. In NDs the protein is misfolded, it shows an increase in the β-sheet structure getting into a pathologic aggregate-fibrillar state. The misfolded protein, at the beginning, gives small oligomers that increase in size till they form large aggregates. The aggregates of all sizes are toxic for cells, and thus for neurons, and they lead to neural damage [2]. On the other hand, the neural damage activates the amyloid precursor proteins involved in the cells signalling driven by synapse retraction, which in turn induce an increase in the amyloid-β production [4]. Thus, amyloid-β synaptotoxicity drives amyloid-β production in a positive feedback loop.

Several mathematical models have been proposed to investigate the biological processes underlying NDs at different scale. At a microscopic level, Smoluchowski equations are often used to describe the self-association among monomers and polimers of different sizes for describing the elongation of fibrils by end-to-end formation[5–8]. Further models include the role of prions ([9]), the growth kinetics of amyloids [10–12], and the use of network-approaches to understanding the behaviour of different brain regions [13, 14]. At the macroscopic level, the spreading of neural damages is typically modelled

through a nonlinear reaction-diffusion mechanism [15, 16], that can be effectively coupled with nucleation-aggregation-fragmentation models for the dynamics in the brain connectome [17, 18]. Multiscale approaches have been proposed in [19–21], assuming that the damage diffuses in the neuronal net through a neuron-to-neuron prion-like propagation mechanism and that monomeric form of the amyloid spreads through the brain tissue undergoing agglomeration.

The aim of this work is to bridge the gap between microscopic and macroscopic approaches proposing a toy partial differential model able to take into account both for the short-time dynamics of the misfolded proteins aggregating in plaques and the long-term evolution of neural damage. In particular, we are focused on modeling the evolution of the disease starting from a delimited brain region presenting an hoarding of amyloid-β and amyloid precursor proteins. The article is organised as follows. In Section 2, we introduce the mathematical model and in Section 3 we perform its dimensional analysis. In Section 4, we describe its numerical implementation and we discuss the numerical results in few test cases. We also propose two biomarkers to be compared with the ones used for describing the progressing of NDs. In Section 5 we collect few concluding remarks.

2 The mathematical model

We consider the brain tissue as a binary, saturated, closed and incompressible mixture composed by a protein phase of proliferating plaques and a healthy phase representing the host tissue. Let ϕ_p and ϕ_t be the volume fraction of the plaques and the healthy tissue, respectively. Assuming that both phases have the same mass density γ, the following

continuity equations hold:

$$\begin{aligned} \frac{\partial \phi_p}{\partial t} + \nabla \cdot (\phi_p \mathbf{v}_p) &= \frac{S_p}{\gamma} + \nabla \cdot \mathbf{k}_p, \\ \frac{\partial \phi_t}{\partial t} + \nabla \cdot (\phi_t \mathbf{v}_t) &= \frac{S_t}{\gamma} + \nabla \cdot \mathbf{k}_t, \end{aligned} \tag{1}$$

where $\mathbf{v}_i$, with $i = (p, t)$, is the velocity of the i-th phase, S_i is the volumetric source term and $\mathbf{k}_i$ is the non-convective mass flux. The mixture is saturated, i.e.

$$\phi_p + \phi_t = 1, \tag{2}$$

and it is not growing, i.e.

$$S_p + S_t = 0; \qquad \mathbf{k}_p + \mathbf{k}_t = \mathbf{0}. \tag{3}$$

in order to locally satisfy the conservation of mass exchanged between the phases. Accordingly, the continuity equation for the whole mixture obtained summing up the two equations in (1) reads:

$$\nabla \cdot (\phi_p \mathbf{v}_p + \phi_l \mathbf{v}_t) = 0. \tag{4}$$

Following [22, 23], we use the principle of maximum dissipation to obtain the constitutive laws for phase velocities. In particular, we aim to find the stationary values of the Rayleghian $\mathfrak{R}$, defined as:

$$\mathfrak{R} = W + \frac{dE}{dt}, \tag{5}$$

where W is the energy dissipation and E is the Landau free energy of the system. We assume that the main dissipation source is given by the viscous interactions due to the

relative motion between the phases, i.e.

$$W = \frac{1}{2}\int_{\Omega} \phi_p(\mathbf{v}_p - \mathbf{v}_t)^T \mathbf{M}(\mathbf{v}_p - \mathbf{v}_t) dV, \tag{6}$$

where $\mathbf{M} = M_0 \mathbf{T}^{-1}$, is a tensor representing volumetric friction, that is inversely proportional to the preferential directions tensor $\mathbf{T}$, M_0 is a friction parameter, and Ω represents the whole brain. The tensor $\mathbf{T}$ takes into account for the local anisotropy of the brain micro-structure, and it can be extracted from clinical neuroimaging data, such as diffusion tensor imaging.

The Landau free energy E reads:

$$E = \int_{\Omega} \left(\frac{\gamma_\phi^2}{2} |\nabla \phi_p|^2 + \Psi(\phi_p) \right) dV, \tag{7}$$

where $\Psi(\phi_p)$ is a local interaction potential of the Lennard-Jones type, while the quadratic gradient terms is a short-range nonlocal potential governed by the small parameter γ_ϕ. In particular, we assume that $\Psi(\phi_p)$ has the form:

$$\Psi(\phi_p) = F \frac{\phi_p^2(\phi_p - \phi_e)}{1 - \phi_p},$$

where F is a characteristic interaction energy density. Since $\Psi(\phi_p)$ is non-convex, the gradient term in (7) acts as a regularizing effect that creates a diffuse interface between region with higher and lower concentration of plaques. Assuming that the mixture is highly viscous and that the tissue behaves as a perfect fluid, following [24] we derive a

Cahn-Hilliard type equation for the plaque concentration:

$$\begin{cases} \dfrac{\partial \phi_p}{\partial t} = \nabla \cdot \left(\dfrac{\phi_p (1-\phi_p)^2}{M_0} \mathbf{T} \nabla \mu \right) + \dfrac{S_p}{\gamma} + \nabla \cdot \mathbf{k}_p, \\ \mu = \frac{\partial \Psi_\phi}{\partial \phi} - \gamma_\phi^2 \Delta \phi. \end{cases} \tag{8}$$

We now have to define the constitutive equation for the source terms in Eq.(8). Following [19], we hypothesize that the damage diffuses in the neuronal net through a neuron-to-neuron prion-like propagation mechanism and that monomeric form of the protein spreads through the microscopic tortuousness of the brain tissue undergoing agglomeration. Eventually this leads to the formation of long, insoluble fibrils, accumulating in spherical deposits known as senile plaques that become toxic for neurons, creating a spreading brain damage. Therefore, we introduce a variable n defining the neuronal damage in the brain, and we assume that the non-convective mass flux is due to chemotactic motion of plaques with respect to the gradient of the neuronal damage, such as:

$$\mathbf{k}_p = k_n \phi_p \mathbf{T} \nabla n \tag{9}$$

where k_n is the chemotactic coefficient.

Similarly, we assume that the volumetric source of plaques is proportional to the local concentration p of precursor proteins, such as amyloid precursor proteins, such that:

$$S_p = \nu_p \gamma \phi_p \left(\frac{p}{p_s} - \delta \right) (1 - \phi_p), \tag{10}$$

where ν_p is the plaque proliferation rate, p_s is the physiological concentration of precursor proteins in the brain tissue and δ is a threshold value, which sets the lower value over

which there is an over accumulation of precursor proteins. The growth of plaques follows a logistic law, with saturation when the plaques occupy all the available volume for $\phi_p = 1$.

We assume that the precursor proteins undergo a reaction-diffusion dynamics, being:

$$\frac{\partial p}{\partial t} = D_p \nabla \cdot (\mathbf{T} \nabla p) + S_n((1-n)\chi_C + n)(p_s - p) - \delta_p \phi_p p. \tag{11}$$

Here, we are assuming that there is a region Ω_C in which initially there is a hoarding of precursor proteins and where the plaques formation begins, with χ_C its indicator function. Outside of Ω_C, damage propagation triggers the accumulation of precursor proteins, which enhances the formation of plaques, thus modeling the pathogenic positive feedback loop between amyloid production and synapse damage reported in literature [4] Hence, the source term $S_n\beta((1-n)\chi_C + n)(p_s - p)$ describes the growth rate of precursor proteins in Ω_C and in regions where the neural damage propagates. δ_p is the consumption rate of proteins by the plaques.

Moreover, assuming that $\hat{n}$ propagates following the same pathway of the electrical signal in the brain, we describe the neural damage dynamics as follows:

$$\begin{aligned} \frac{\partial n}{\partial t} = \epsilon D_n \nabla \cdot (\mathbf{D} \nabla n) - \epsilon K_n n(n-1)(n-\alpha) + \\ \epsilon C_s \chi_{C_n}(K(\phi_p) - \delta_n)(1-n). \end{aligned} \tag{12}$$

Indeed, Equation (12) is an Allen-Cahn type equation, often adopted to model the signal propagation in presence of damage [25]. Here, the neural damage is taken into account by the term $\epsilon C_s \chi_{C_n}(K(\phi_p) - \delta_n)(1-n)$, where $K(\phi_p)$ is the fractional area occupied by the plaques in Ω_C and defined as $K(\phi_p) = \frac{\int_{\Omega_C} I_{(\phi_p > 0.3)}}{\int_{\Omega_C} d\Omega}$. Moreover, χ_{C_n} represents a gaussian supported over the circular damaged area, giving the maximum damage onset in its center, δ_n is the threshold above which the plaques create neuronal damage and

C_s is the neural damage proliferation rate. Moreover, we include a small dimensionless parameter ϵ accounting for the fact that the spreading dynamics of the neural damage is much slower than the dynamics of protein misfolding and agglomeration. On the other hand, the bidimensional propagation is described from the first two terms at the right hand side of Equation (12), where D_n is a diffusion coefficient, $\mathbf{D}$ is the tensor of the preferential directions of the expansion of damage and K_n is a sink proliferation rate. We further remark that the term α is required to belong to the range $(0, \frac{1}{2})$ in order to allow the existence of a travelling wave solution.

3 Dimensional analysis

The partial differential model is made by eqs. (8, 11,12) equipped with no-flux conditions for the variables ϕ_p, μ, n, p on the brain boundary. We first remark that the partial differential system has multiple time-scales, namely:

- the phase separation and coarsening of ϕ_p, i.e. $t_1 \sim \epsilon \frac{M_0 \gamma_\phi^2}{F^2}$;
- the proliferation rate of ϕ_p, i.e. $t_2 \sim \frac{\epsilon}{\nu_p}$;
- the interaction between the precursor protein and the plaques, i.e. $t_3 \sim \frac{M_0 D_p}{F \delta_p}$
- the diffusion of n, i.e. $t_4 \sim \frac{F}{\epsilon M_0 \nu_p D_n}$;
- the proliferation rate of the neuronal damage, i.e. $t_5 \sim \frac{1}{\epsilon C_S}$

For the sake of simplicity, let us first introduce the following dimensionless variables:

$$\hat{p} = \frac{p}{p_s}, \qquad \hat{n} = n, \qquad \hat{\mu} = \frac{\mu}{F}, \qquad \hat{t} = t\nu_p, \qquad \hat{x} = x\sqrt{\frac{\delta_p}{D_p}}.$$

After standard manipulations we obtain the following dimensionless system:

$$\begin{cases} \dfrac{\partial \phi_p}{\partial \hat{t}} = \hat{D}\hat{\nabla}\cdot\left(\phi_p(1-\phi_p)^2\mathbf{T}\hat{\nabla}\hat{\mu}\right)+\phi_p(\hat{p}-\delta)(1-\phi_p)+\hat{k}\hat{\nabla}\cdot(\phi_p\mathbf{T}\hat{\nabla}\hat{n}) \\ \hat{\mu} = \hat{f}-\hat{\gamma}_\phi\hat{\Delta}\phi_p \\ \dfrac{\partial \hat{p}}{\partial \hat{t}} = \hat{\nu}\left(\hat{\nabla}\cdot(\mathbf{T}\hat{\nabla}\hat{p})+\hat{\beta}((1-\hat{n})\chi_C+\hat{n})(1-\hat{p})-\phi_p\hat{p}\right) \\ \dfrac{\partial \hat{n}}{\partial \hat{t}} = \epsilon\hat{D}_n\hat{\nabla}\cdot(\mathbf{D}\hat{\nabla}\hat{n})-\epsilon\hat{K}_n\hat{n}(\hat{n}-1)(\hat{n}-\alpha)+\epsilon\hat{C}_s\chi_{C_n}(K(\phi_p)-\delta_n)(1-\hat{n}) \end{cases} \tag{13}$$

that is governed by the following dimensionless parameters:

$$\hat{D}=\frac{F\delta_p}{\nu_p D_p M_0},\quad \hat{k}=\frac{\delta_p k_n}{D_p\nu_p},\quad \hat{\gamma}_\phi=\frac{\gamma_\phi^2\delta_p}{D_p F},\quad \hat{\nu}=\frac{\delta_p}{\nu_p},$$

$$\hat{f}=\frac{1}{F}\frac{\partial\Psi_\phi}{\partial\phi},\quad \beta=\frac{S_p}{\delta_p},\quad \hat{D}_n=\frac{D_n\delta_p}{\nu_p D_p},\quad \hat{K}_n=\frac{K_n}{\nu_p},\quad \hat{C}_s=\frac{C_s}{\nu_p},\quad \epsilon.$$

4 Numerical results

4.1 Finite element implementation

The dimensionless model in (13) is numerically solved using the library FreeFEM++ for solving partial differential equations using finite element method [26]. The finite element approximation of the model preserves the physical bounds for the variables representing plaques and the neural damage, that are non-negative and smaller or equal to one. Moreover, the introduction of the degenerate mobility in the Cahn-Hilliard equation makes the solution not unique. In the numerical formulation we go beyond the last issue introducing a subdivision of the nodes of the mesh domain into active and passive nodes, following

[27, 28]. The lumping approximation of the mass scalar products in the finite element discretization is introduced in order for the discrete solution to be able to track compactly supported solutions of Cahn-Hilliard equation with a free boundary which moves with a finite speed. This method allows to select the physical solutions with compact support and moving boundary. Moreover we have taken into account both for the dissipative behaviour of the system, that is not preserved at the discrete level, by introducing a splitting of the energy functional into a convex and a concave part, and for the positivity of the ϕ_p by imposing a variational inequality following the algorithm proposed in [29]. The associated gradient projection algorithm is formulated in terms of a backtracking line search method, in order to optimize the choice of the descent coefficient, using the Armijo method [30], based on the Armijo-Goldstein condition as in algorithm proposed by [31]. Moreover we developed a time step adaptivity procedure for taking into account for all the time scales of the system dynamics, from the phase separation of the plaques to the spread of neural damage.

Finally, we performed numerical simulations on a two dimensional circular domain centred in the origin with a dimensionless diameter equal to 100. Since we set the characteristic length to $\sqrt{(D_n/\delta_n)} = 0.1\ mm$, it corresponds to a physical domain whose diameter is of 1 cm. We subdivided the domain in triangles, choosing 124 elements for each side in order to evaluate the plaques formation and the neural damage propagation and we used continuous linear elements. We fix the values of the dimensionless parameters as $\epsilon = 0.1$, $\hat{D} = 4.48$, $\hat{\gamma}_\phi = 0.03$, $\hat{\nu} = 1000$, $\hat{\beta} = 0.045$, $\hat{K}_n = 10\epsilon$, $\hat{C}_s = 5.5$, $\beta = 0.045$, $\alpha = 0.2$, $\delta = \delta_n = 0.3$, $\phi_e = 0.6$, while we vary the values of $\hat{D}_n$ and $\hat{k}$ in the following test cases. The time step is set to $\Delta t = 0.5\ \hat{\gamma}_\phi^2$ for the first iteration and then it is determined step by step through the adaptive procedure. We choose the initial conditions $n(\mathbf{x}, 0) = n_0(\mathbf{x}) = 0$, $p(\mathbf{x}, 0) = p_0(\mathbf{x}) = \chi_C$ and $\phi_p(\mathbf{x}, 0) = \phi_0(\mathbf{x}) = (0.18 + 0.018 \cdot (1 - 2r))\chi_C$, where r is a

random number sampled from the uniform distribution over $[0, 1]$ and χ_C is the indicator function of the subdomain Ω_C, a circle centered at the middle of the domain with a dimensionless diameter equal to 25.

4.2 Numerical simulations

We performed numerical simulations varying the dimensionless parameters $\hat{k}$, $\hat{D}_n$ in order to investigate the effects on the dynamics of the chemotaxis and of the diffusion of the neural damage, respectively. We also simulated two different cases of material microstructure, being:

- isotropic case, i.e. $\mathbf{T} = \mathbf{D} = \text{diag}(1,\ 1)$;
- anisotropic case, i.e $\mathbf{D} = \text{diag}(1,\ 20)$ and $\mathbf{T} = \text{diag}(0.1,\ 1.9)$.

We performed the first set of simulations by imposing $\hat{k} = 2.5$, $\hat{D}_n = 1$, exploring both the isotropic and anisotropic scenarios. The early stage dynamics is about the same for both the two cases. As depicted in Figure 1, we first observe the phase separation of the solution for ϕ_p, followed by a clustering dynamics without any formation of neuronal damage. We observe no significant qualitative difference between the isotropic and the anisotropic case.

The later stage dynamics for the isotropic case is depicted in Figure 2. Once the plaque clusters are completely formed, the neural damage begins to expand. The plaques later spread through the healthy tissue following the radial direction of the damage growth, while the inner region becomes completely damaged.

Figure 3 displays the numerical results for the anisotropic case, simulated with the same parameters values of the previous isotropic case, i.e. $\hat{k}_n = 2.5$, $\hat{D}_n = 1$. In this latter case, the neural damage starts growing at about $\hat{t} = 11.7$ and it immediately

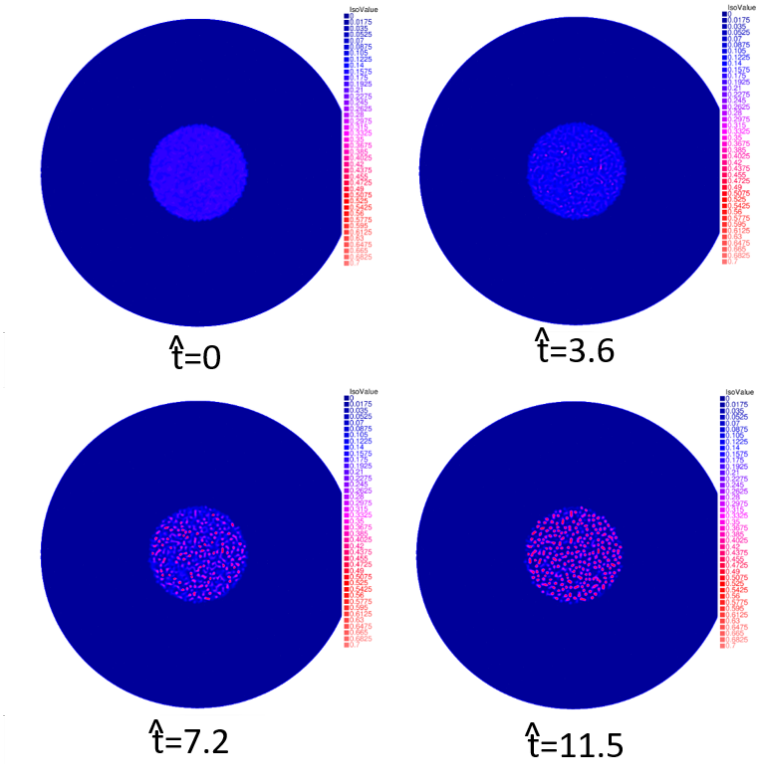

Figure 1: Colormap of the spatial distribution of ϕ_p during the early stage dynamics, shown at $\hat{t} = 0$, 3.6, 7.2, 11.5 setting $\hat{k} = 2.5$, $\hat{D}_n = 1$.

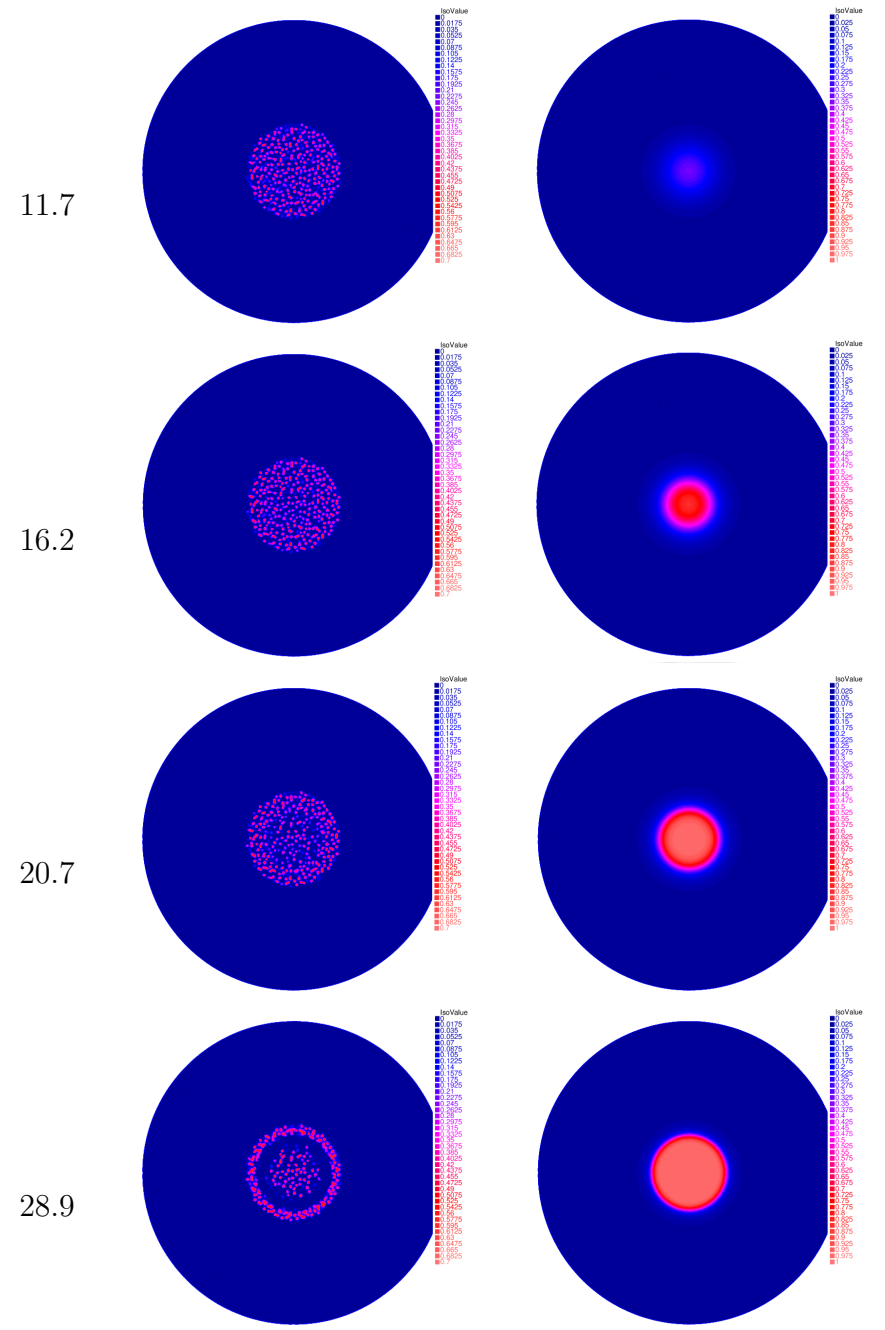

Figure 2: Colormap of the spatial distribution of ϕ_p and $\hat{n}$ during the later stages of dynamics, shown at $\hat{t} = 11.7, 16.2, 20.7, 28.9$ setting $\hat{k} = 2.5$, $\hat{D}_n = 1$ for the isotropic case.

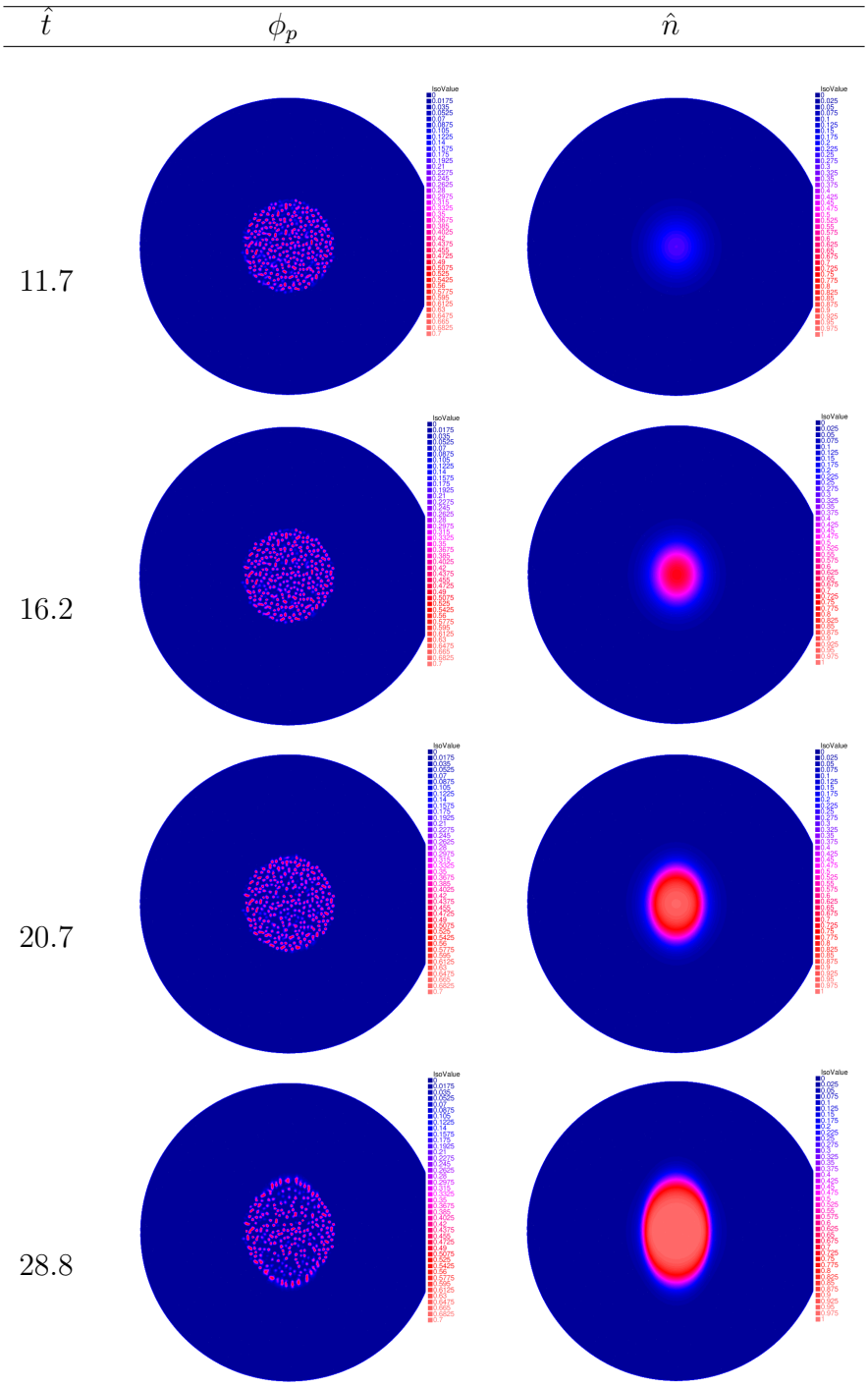

Figure 3: Colormap of the spatial distribution of ϕ_p and $\hat{n}$ during the later stages of dynamics, shown at $\hat{t} = 11.7$, 16.2, 20.7, 28.9 setting $\hat{k} = 2.5$, $\hat{D}_n = 1$ for the anisotropic case.

follows the preferential direction of the mobility tensor $\mathbf{T}$, followed by the plaques. At the final step, we observe that both the damaged area and the plaque domain take an elliptic shape, highlighting the pivotal importance of the microstructure on the invasion dynamics.

We finally performed another set of simulations for both the isotropic and anisotropic cases. In this case, we increased of an order of magnitude the values of both the chemotactic and the damage diffusion parameters, thus setting $\hat{k} = 25$, $\hat{D}_n = 10$. We find that the initial stage dynamics is qualitatively the same observed in the previous cases, as expected, since $\hat{n}$ has a slow dynamics and its onset is completely determined by the phase separation dynamics of the Cahn-Hilliard equation without the chemotaxis term. A considerable difference from the previous scenarios can be appreciated from the simulation results collected in Figure 4 and Figure 5, for the isotropic and anisotropic cases respectively. In particular, we remark that increasing $\hat{D}_n$ makes the neural damage propagating faster, whilst increasing $\hat{k}$ makes the plaques moving faster towards the front of the neural damage wave.

4.3 Biomarkers

In order to provide a biological interpretation of our numerical results, we present here two biomarkers suitable for quantifying the accumulation of plaques and the extent of neurodegeneration, to be compared to the well known Jack curves [32].

In a clinical setting, a first biomarker is sought to investigate the plaque accumulation. For the Alzheimer Disease, such indicator can be identified with the CSF-Aβ_{42} and the amyloid PET. On the other hand, a second biomarker is used to describe the neurodegeneration since plaques can grow logistically reaching the saturation even decades

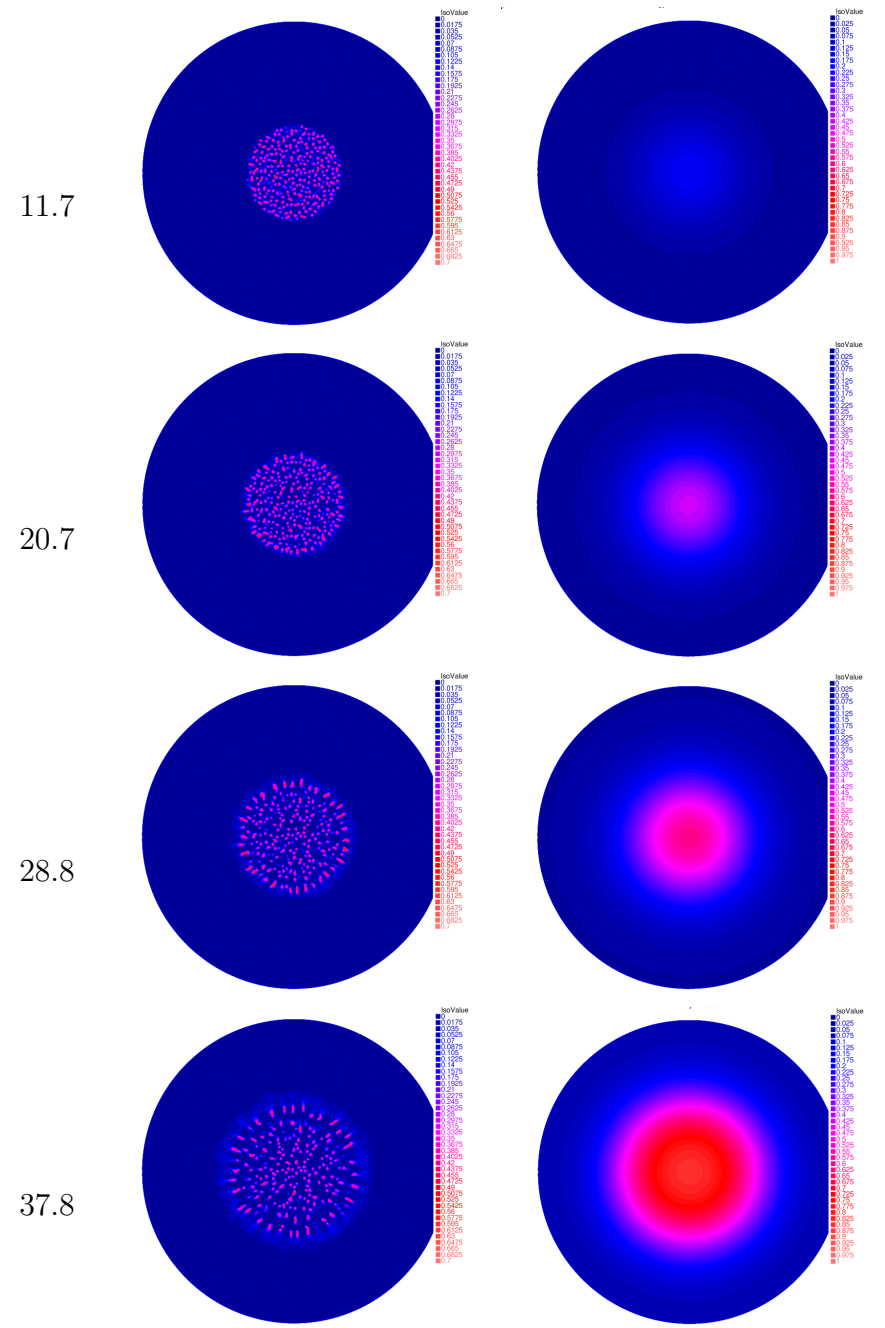

Figure 4: Colormap of the spatial distribution of ϕ_p and $\hat{n}$ during the later stages of dynamics, shown at $\hat{t} = 11.7, 20.7, 28.8, 37.8$ setting $\hat{k} = 25$, $\hat{D}_n = 10$ for the isotropic case.

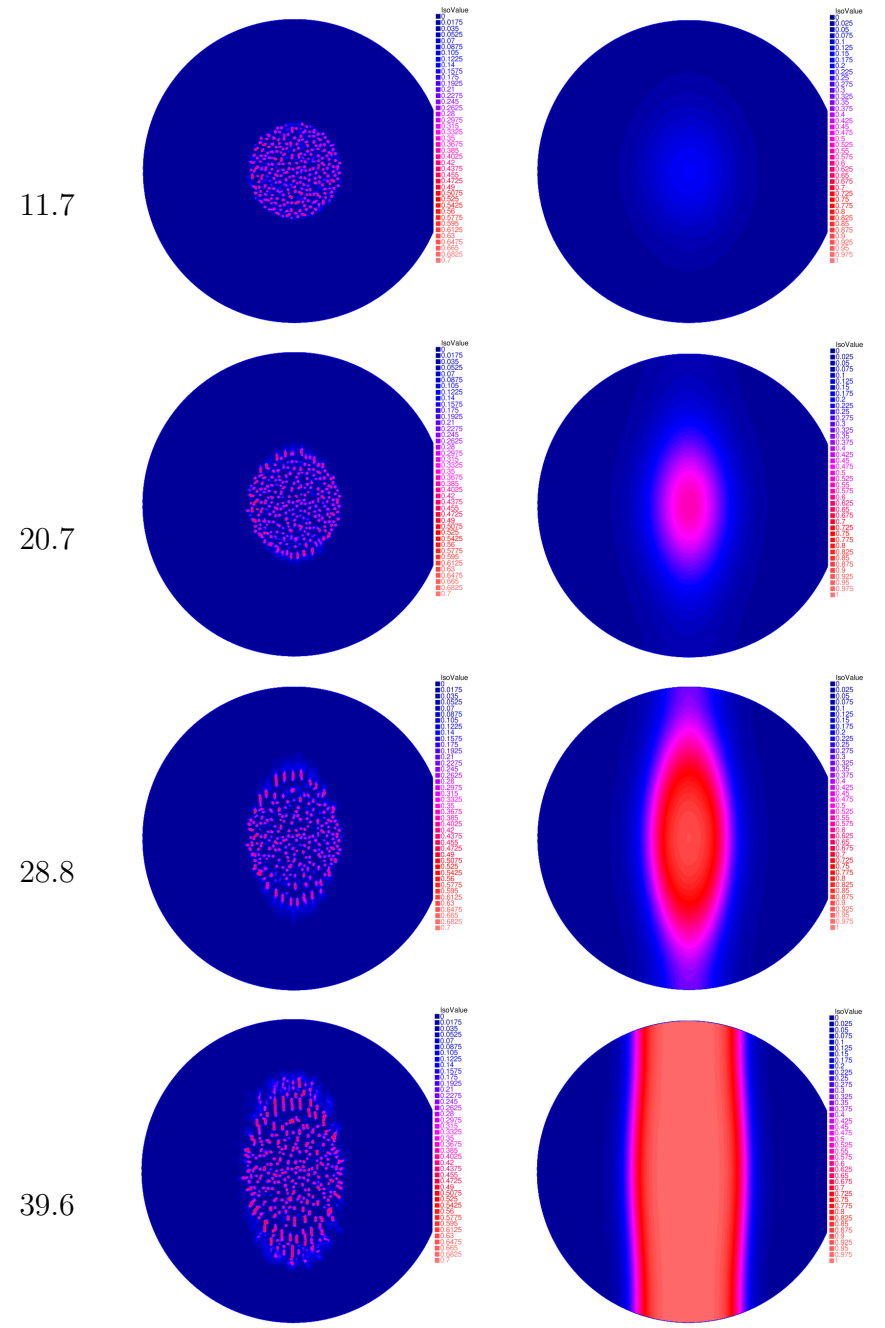

Figure 5: Colormap of the spatial distribution of ϕ_p and $\hat{n}$ during the later stages of dynamics, shown at $\hat{t} = 11.7$, 20.7, 28.8, 37.8 setting $\hat{k} = 25$, $\hat{D}_n = 10$ for the anisotropic case.

before the patient experiences the first symptoms and before MRI or PET detect neuronal damage. Concerning this latter indicator, FDG-PET has been proven to be a promising modality for detecting functional brain changes in AD [33]. The evolution curves of both biomarkers are characterized by a sigmoidal shape with a large time shift.

Accordingly, here we propose two biomarkers for evaluation the simulated dynamics. Firstly, we define the average neural damage as:

$$B_n = \frac{\int_\Omega \hat{n}(x,t)dx}{\int_\Omega dx}, \tag{14}$$

that is a measure of brain atrophy. Secondly, we define the average concentration of plaques over the whole computational domain as:

$$B_p = \frac{\int_\Omega I_{\phi_p>0.3}dx}{\int_\Omega dx}, \tag{15}$$

where $I_{\phi_p>0.3}$ is the indicator function introduced in Section 2.

In Figure 6, we report the evolution of the two biomarkers B_n and B_p, normalized with respect to their maximum value, over the dimensional time t expressed in units of years. We observe that for both the isotropic and the anisotropic case, B_p grows earlier and faster than B_n, presenting the characteristic sigmoidal trend.

On the other hand, B_n starts growing over time as soon as B_p saturates, thus presenting a delay over time with respect to plaques deposition. Finally, we remark that the curves for B_n are not sigmoidal as one should expect. This discrepancy from the clinical results is due to the fact that, to avoid excessive computational costs, we observe B_n over a time interval shorter than the characteristic time of brain atrophy complete development.

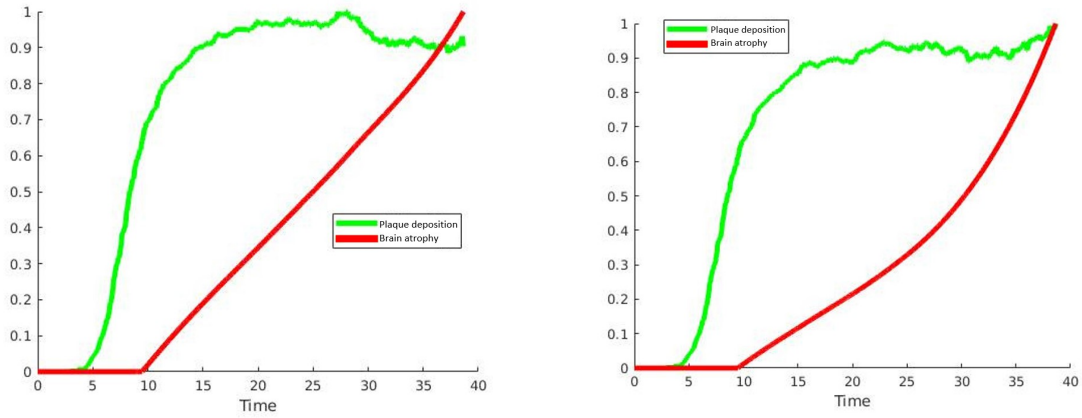

Figure 6: Evolution of the normalised biomarkers B_p (green) and B_n (red) over the dimensional time expressed in years for both the the isotropic (left) and anisotropic (right) case, setting $\hat{k} = 2.5$, $\hat{D}_n = 1$.

5 Conclusion

In this work we developed a toy model for describing both the short-time dynamics of misfolded protein aggregation in plaques and the long-term evolution of neural damage.

Using the theoretical framework of mixtures theory, we considered the brain as a biphasic material made of misfolded protein aggregates, interacting with a local Lennard-Jones potential and a nonlocal short-range term, and of healthy tissue behaving as a perfect fluid. The resulting Cahn-Hilliard type equation for the misfolded proteins contains a growth term depending on the local availability of precursor proteins, that follow a reaction-diffusion equation. The misfolded proteins also posses a chemotactic mass flux driven by gradients of neural damage, that is caused by local accumulation of misfolded protein and that evolves slowly according to an Allen-Cahn equation.

The partial differential model made by Equations (8, 11,12) has been solved numerically using the finite element method in a simple two-dimensional domain, evaluating the effects of the mobility of the misfolded protein and the diffusion of the neural damage.

We considered both isotropic and anisotropic mobility coefficients, highlighting that the spreading front of the neural damage follows the direction of the largest eigenvalue of the mobility tensor. In both cases, we computed two biomarkers to quantify the aggregation in plaques and the evolution of neural damage, that are in qualitative agreement with the characteristic Jack curves for many NDs.

This toy model is a preliminary attempt to build a bridge between microscopic and macroscopic descriptions of NDs covering both the short- and long-time dynamics. As such, it suffers several limitations, as the lack of a realistic polymerization kinetics of the misfolded proteins and of their neuron-to-neuron prion-like propagation mechanism. This modeling aspect must be addressed in the future in order to the model relevant for the biological research community. Notwithstanding, the possibility to integrate patient-specific data of diffusion tensor imaging into the tensors of diffusion and mobility may pave the way to identify the preferred spreading pathways of the neural damage depending on the specific brain architecture, possibly leading to the creation of a predictive tool helping the clinician in the early screening of the pathology.

Acknowledgements

This work was supported by MUR PRIN 2017 grant 2017KL4EF3, by Regione Lombardia project NEWMED (Grant No. POR FESR 2014-2020) and partly by GNFM – INdAM through the program *Progetto Giovani 2020*.

References

[1] M. Jucker and L. C. Walker. "Self-propagation of pathogenic protein aggregates in neurodegenerative diseases." In: *Nature* 501.7465 (2013), pp. 45–51.

[2] C. Soto and S. Pritzkow. "Protein misfolding, aggregation, and conformational strains in neurodegenerative diseases." In: *Nature neuroscience* (2018), p. 1.

[3] M. Jucker and L. C. Walker. "Propagation and spread of pathogenic protein assemblies in neurodegenerative diseases." In: *Nature neuroscience* 21.10 (2018), p. 1341.

[4] C. Elliott et al. "A role for APP in Wnt signalling links synapse loss with β-amyloid production." In: *Translational psychiatry* 8.1 (2018), pp. 1–13.

[5] M. M. Pallitto and R. M. Murphy. "A mathematical model of the kinetics of β-amyloid fibril growth from the denatured state." In: *Biophysical journal* 81.3 (2001), pp. 1805–1822.

[6] D. L. Craft, L. M. Wein, and D. J. Selkoe. "A Mathematical Model of the Impact of Novel Treatments on the AβBurden in the Alzheimer's Brain, CSF and Plasma." In: *Bulletin of mathematical biology* 64.5 (2002), pp. 1011–1031.

[7] L. Edelstein-Keshet and A. Spiros. "Exploring the formation of Alzheimer's disease senile plaques in silico." In: *Journal of theoretical biology* 216.3 (2002), pp. 301–326.

[8] B. Franchi and M. C. Tesi. "A qualitative model for aggregation-fragmentation and diffusion of β-amyloid in Alzheimer's disease." In: *Rend. Semin. Mat. Univ. Politec. Torino* 70 (2012), pp. 75–84.

[9] M. Helal et al. "Alzheimer's disease: analysis of a mathematical model incorporating the role of prions." In: *Journal of mathematical biology* 69.5 (2014), pp. 1207–1235.

[10] B. Franchi and S. Lorenzani. "From a microscopic to a macroscopic model for Alzheimer disease: two-scale homogenization of the Smoluchowski equation in perforated domains." In: *Journal of Nonlinear Science* 26.3 (2016), pp. 717–753.

[11] M. Bertsch et al. "Microscopic and macroscopic models for the onset and progression of Alzheimer's disease." In: *Journal of Physics A: Mathematical and Theoretical* 50.41 (2017), p. 414003.

[12] L. Desvillettes and S. Lorenzani. "Homogenization of the discrete diffusive coagulation–fragmentation equations in perforated domains." In: *Journal of Mathematical Analysis and Applications* 467.2 (2018), pp. 1100–1128.

[13] F. Matthäus. "The spread of prion diseases in the brain—models of reaction and transport on networks." In: *Journal of Biological Systems* 17.04 (2009), pp. 623–641.

[14] Y. Iturria-Medina et al. "Epidemic spreading model to characterize misfolded proteins propagation in aging and associated neurodegenerative disorders." In: *PLoS computational biology* 10.11 (2014), e1003956.

[15] J. Weickenmeier, E. Kuhl, and A. Goriely. "Multiphysics of prionlike diseases: Progression and atrophy." In: *Physical review letters* 121.15 (2018), p. 158101.

[16] J. Weickenmeier et al. "A physics-based model explains the prion-like features of neurodegeneration in Alzheimer's disease, Parkinson's disease, and amyotrophic lateral sclerosis." In: *Journal of the Mechanics and Physics of Solids* 124 (2019), pp. 264–281.

[17] S. Fornari et al. "Prion-like spreading of Alzheimer's disease within the brain's connectome." In: *Journal of the Royal Society Interface* 16.159 (2019), p. 20190356.

[18] S. Fornari et al. “Spatially-extended nucleation-aggregation-fragmentation models for the dynamics of prion-like neurodegenerative protein-spreading in the brain and its connectome.” In: *Journal of theoretical biology* 486 (2020), p. 110102.

[19] M. Bertsch et al. “Alzheimer’s disease: a mathematical model for onset and progression.” In: *Mathematical medicine and biology: a journal of the IMA* 34.2 (2016), pp. 193–214.

[20] M. Bertsch et al. “Alzheimer’s disease: a mathematical model for onset and progression.” In: *Mathematical medicine and biology: a journal of the IMA* 34.2 (2017), pp. 193–214.

[21] A. Goriely, E. Kuhl, and C. Bick. “Neuronal oscillations on evolving networks: Dynamics, damage, degradation, decline, dementia, and death.” In: *Physical review letters* 125.12 (2020), p. 128102.

[22] M. Doi and A. Onuki. “Dynamic coupling between stress and composition in polymer solutions and blends.” In: *Journal de Physique II* 2.8 (1992), pp. 1631–1656.

[23] S. M. Wise et al. “Three-dimensional multispecies nonlinear tumor growth—I: model and numerical method.” In: *Journal of theoretical biology* 253.3 (2008), pp. 524–543.

[24] C. Chatelain et al. “Emergence of microstructural patterns in skin cancer: a phase separation analysis in a binary mixture.” In: *New Journal of Physics* 13.11 (2011), p. 115013.

[25] J. P. Keener and J. Sneyd. *Mathematical physiology 1: Cellular physiology*. 2009.

[26] F. Hecht. “New development in FreeFem++.” In: *Journal of Numerical Mathematics* 20.3-4 (2012), pp. 251–265.

[27] J. Barrett and J. Blowey. "Finite element approximation of the Cahn-Hilliard equation with concentration dependent mobility." In: *Mathematics of Computation of the American Mathematical Society* 68.226 (1999), pp. 487–517.

[28] A. Agosti et al. "A Cahn-Hilliard–type equation with application to tumor growth dynamics." In: *Mathematical Methods in the Applied Sciences* 40.18 (2017), pp. 7598–7626.

[29] J. W. Barrett, J. F. Blowey, and H. Garcke. "Finite Element Approximation of the Cahn–Hilliard Equation with Degenerate Mobility." In: *SIAM Journal on Numerical Analysis* 37.1 (1999), pp. 286–318.

[30] C. T. Kelley. *Iterative methods for optimization*. SIAM, 1999.

[31] V. Acary and B. Brogliato. *Numerical methods for nonsmooth dynamical systems: applications in mechanics and electronics*. Springer Science & Business Media, 2008.

[32] J. Jr Clifford et al. "Tracking pathophysiological processes in Alzheimer's disease: an updated hypothetical model of dynamic biomarkers." In: *The Lancet Neurology* 12.2 (2013), pp. 207–216.

[33] L. Mosconi et al. "Pre-clinical detection of Alzheimer's disease using FDG-PET, with or without amyloid imaging." In: *Journal of Alzheimer's Disease* 20.3 (2010), pp. 843–854.

MOX Technical Reports, last issues

Dipartimento di Matematica
Politecnico di Milano, Via Bonardi 9 - 20133 Milano (Italy)

10/2022 Fresca, S.; Manzoni, A.
Real-time simulation of parameter-dependent fluid flows through deep learning-based reduced order models

09/2022 Corti, M.; Zingaro, A.; Dede', L.; Quarteroni, A.
Impact of Atrial Fibrillation on Left Atrium Haemodynamics: A Computational Fluid Dynamics Study

07/2022 Sinigaglia, C.; Quadrelli, D.E.; Manzoni, A.; Braghin, F.
Fast active thermal cloaking through PDE-constrained optimization and reduced-order modeling

06/2022 Pozzi, G.; Grammatica, B.; Chaabane, L.; Catucci, M.; Mondino, A.; Zunino, P.; Ciarletta, P.
T cell therapy against cancer: a predictive diffuse-interface mathematical model informed by pre-clinical studies

08/2022 Gobat, G.; Opreni, A.; Fresca, S.; Manzoni, A.; Frangi, A.
Reduced order modeling of nonlinear microstructures through Proper Orthogonal Decomposition

05/2022 Aspri, A; Beretta, E.; Cavaterra, C.; Rocca, E.; Verani, M.
Identification of cavities and inclusions in linear elasticity with a phase-field approach

04/2022 Africa, P.C.; Piersanti, R.; Fedele, M.; Dede', L.; Quarteroni, A.
lifex - heart module: a high-performance simulator for the cardiac function

01/2022 Gavazzoni, M.; Ferro, N.; Perotto, S.; Foletti, S.
Multi-physics inverse homogenization for the design of innovative cellular materials: application to thermo-mechanical problems

03/2022 Giacomini, M.; Perotto, S.
Anisotropic mesh adaptation for region-based segmentation accounting for image spatial information

02/2022 Antonietti, P.F.; Scacchi, S.; Vacca, G.; Verani, M.
C^1-VEM for some variants of the Cahn-Hilliard equation: a numerical exploration